Bulletin of the Seismological Society of America, Vol. 100, No. 6, pp. 3174–3182, December 2010, doi: 10.1785/0120100030

Maximum-Likelihood Method for Estimating Coda Q and the Nakagami-m Parameter

by Hisashi Nakahara and Eduard Carcolé

Abstract We propose a new method to simultaneously estimate coda Q and the Nakagami-m parameter from seismogram envelopes based on the maximum-likelihood (ML) method. Coda Q is a parameter characterizing a smooth decay in seismic coda and is considered to reflect physical parameters in the Earth such as intrinsic absorption, scattering attenuation, and so on. The Nakagami-m parameter, denoted by m, is a shape parameter of the Nakagami-m distribution, which was originally proposed in the 1940s for the purpose of statistically characterizing the fading of short radio waves. Recently, it was found that the statistics of high-frequency seismogram envelopes also obey the Nakagami-m distribution. An ML estimation of coda Q was so far proposed assuming Rayleigh distribution, which is equivalent to the Nakagami-m distribution for $m = 1$. This study extends the previous method for estimating coda Q to the values of m different from 1. Concerning the estimation of m, this study may be the first to propose an ML method for high-frequency seismic waves. From the data analysis of local earthquakes in the frequency range from 1 to 32 Hz, we find that coda Q ranges from 100 at 1–2 Hz to 2000 at 16–32 Hz increasing with frequencies increasing. And the values are compatible with previously reported values. The m-parameter varies with events and is significantly different from 1 for some events. But mean values of m with respect to the events are close to 1 irrespective of components and frequencies. Variations in m are found to be larger for lower frequencies. The m-parameter is exactly equal to a reciprocal of the scintillation index, which is used to express fluctuations in seismogram envelopes. Introduction of the m-parameter into seismology will help investigate statistical characteristics of small-scale fluctuations in seismic velocity structure in the Earth from fluctuations in seismogram envelopes.

Introduction

Fluctuations in amplitude caused by multiple arrivals of waves at the same time are called multipath fading in radio wave propagation. In the 1940s, the Nakagami-m distribution was proposed to describe the statistics of the fading of short radio waves (Nakagami, 1943; Nakagami, 1960). The distribution is still widely used in mobile communications (e.g., Karasawa, 2003). Its probability density function is expressed as

$$p(r) = \frac{2m^m}{\Omega^m \Gamma(m)} r^{2m-1} \exp\left(-\frac{m}{\Omega} r^2\right), \tag{1}$$

where m is the Nakagami-m parameter, Γ is the gamma function, r is amplitude that is calculated from an original time series $u(t)$ and its Hilbert transform $H[u(t)]$ as

$$r(t) = \sqrt{u(t)^2 + H[u(t)]^2}, \tag{2}$$

and $\Omega = E[r^2]$ is an ensemble average of mean squared amplitude. The distribution is able to express different kinds of distributions with changing m from 0.5 to infinity as shown in Figure 1. For example, $m = 0.5$ corresponds to the half Gaussian, and $m = 1$ matches Rayleigh distribution. For the estimation of m, the maximum-likelihood (ML) method is statistically more reasonable than the least squares method because data obey a distribution different from Gaussian. Therefore, the ML estimation method for m was already proposed in 1950s according to Zhang (2002).

In seismology, Ω is known to be time-dependent as shown in Figure 2, and is called mean squared (MS) seismogram envelope. This is a contrast to radio wave propagation in which Ω is assumed to be stationary (time independent). The following functional form for Ω is often used (e.g., Aki and Chouet, 1975):

$$\Omega \propto t^{-k} \exp\left(-\frac{\omega t}{Q_c}\right), \tag{3}$$

where Q_c is the coda Q, t is the lapse time measured from earthquake origin time, ω is the angular frequency, and k is

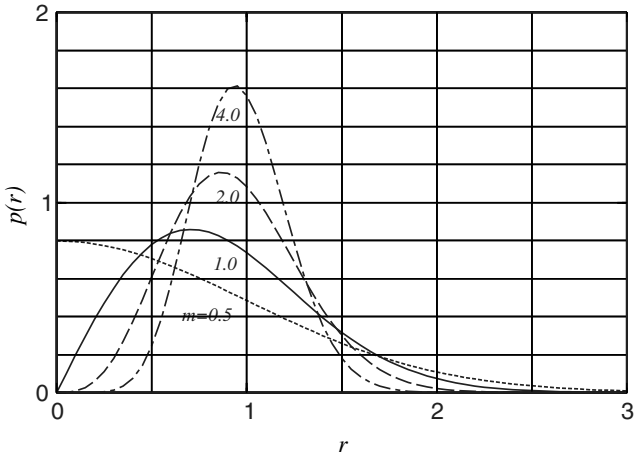

Figure 1. Plot of the probability density functions of the Nakagami-m distribution for different values of m. $\Omega = 1$ is assumed in the plot. $m = 0.5$ corresponds to the half Gaussian, and $m = 1$ matches the Rayleigh distribution. Probability density function becomes 0 at $r = 0$ for $m \geq 1$.

an exponent for the geometrical spreading factor: 2 for body waves and 1 for surface waves. Coda Q is a parameter to characterize a smooth decay in seismogram envelopes and is considered to reflect physical parameters in the Earth such as intrinsic absorption, scattering attenuation (e.g., Sato and Fehler, 1998). For the ML estimation of coda Q, statistics of seismogram envelopes has to be known. Takahara and Yomogida (1992) confirmed that the root mean squared (rms) envelopes obey Rayleigh distribution, which is a special case of $m = 1$. They also proposed an ML estimation method for coda Q based on Rayleigh distribution.

Recently, Carcolé and Sato (2009) have found that fluctuations in seismogram envelopes obey the Nakagami-m distribution. This means that m is sometimes significantly different from 1, and the assumption of Rayleigh distribution is not always appropriate. Therefore, we develop a novel ML method to simultaneously estimate coda Q and the Nakagami-m parameter based on the Nakagami-m distribution. For the estimation of coda Q, the method is an extension of Takahara and Yomogida (1992). This study may be the first to propose an ML estimation method of the m-parameter for seismic waves.

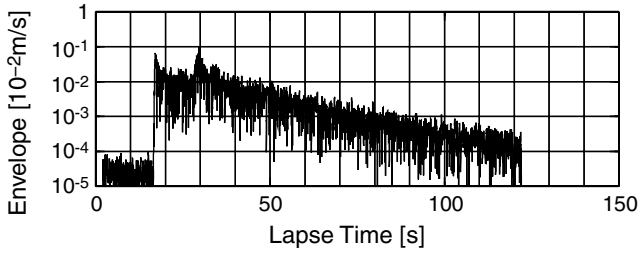

Figure 2. Logarithmic plot of envelope $r(t)$ in 8–16 Hz on the vertical component at IWTH17 station for a local earthquake with a magnitude of 5.2 and a hypocentral distance of about 100 km. The envelope slowly decays with time with superimposing rapid fluctuations.

Method

Maximum-Likelihood Estimation Method of Coda Q and the Nakagami-m Parameter

Here, we derive an ML method to simultaneously estimate coda Q and the Nakagami-m parameter. We express Ω in equation (1) by

$$\Omega = \alpha t^{-k} \exp(-\beta t), \tag{4}$$

where α is a constant controlling amplitude, and β is also a constant for which

$$\beta = \frac{\omega}{Q_c} \tag{5}$$

from equation (3). Here we introduce the following likelihood function by assuming that n sampled amplitudes at times $t_i (i = 1, \ldots, n)$ are mutually independent:

$$L \equiv \prod_{i=1}^{n} p[r(t_i)], \tag{6}$$

where $p[r(t_i)]$ is the probability density function for the Nakagami-m distribution, but its time dependence is explicitly shown here by t_i . The following log-likelihood function is easier to handle:

$$\log L \equiv \sum_{i=1}^{n} \log p[r(t_i)]. \tag{7}$$

We estimate the three unknown parameters α, β, and m by maximizing the log likelihood as:

$$\frac{\partial \log L}{\partial \alpha} = 0, \tag{8a}$$

$$\frac{\partial \log L}{\partial \beta} = 0, \tag{8b}$$

$$\frac{\partial \log L}{\partial m} = 0. \tag{8c}$$

From equations (8a) and (8b), we can derive equations (9) and (10):

$$\frac{1}{n}\left(\sum_{i=1}^{n} t_i\right)\left(\sum_{i=1}^{n} r_i^2 t_i^k \exp(\beta t_i)\right) - \sum_{i=1}^{n} r_i^2 t_i^{k+1} \exp(\beta t_i) = 0. \tag{9}$$

Hereafter, we express $r(t_i)$ as r_i for brevity. We can numerically solve this equation for β as described in detail in the Application to Data section, through which coda

Q is estimated according to equation (5). Once β is obtained, we can estimate α from

$$\hat{\alpha} = \frac{1}{n}\sum_{i=1}^{n} r_i^2 t_i^k \exp(\hat{\beta} t_i), \tag{10}$$

where $\hat{}$ means the estimated value. Here, a notable result is that the estimation of α and β does not depend on the m-parameter. Therefore, the method of Takahara and Yomogida (1992) originally proposed for Rayleigh distribution, the case of $m = 1$, is correct even for the Nakagami-m distribution with other m values.

Using the estimated α and β, m can be estimated by numerically solving

$$n[1 + \log m - \log \hat{\alpha} - \psi(m)] + k\sum_{i=1}^{n} \log t_i + \hat{\beta}\sum_{i=1}^{n} t_i + \sum_{i=1}^{n} \log r_i^2 - \frac{\sum_{i=1}^{n} r_i^2 t_i^k \exp(\hat{\beta} t_i)}{\hat{\alpha}} = 0. \tag{11}$$

Here, the digamma function is defined as

$$\psi(m) \equiv \frac{d \log \Gamma(m)}{dm}. \tag{12}$$

The numerical solution to equation (11) is explained in detail in the Application to Data section.

Error Estimation of the Parameters

How to estimate errors of the three parameters is mentioned here. We introduce the Fisher information matrix that is equivalent to the Hessian matrix of the log-likelihood as

$$[\mathbf{H}(\hat{\boldsymbol{\theta}})]_{ij} = -\left[\frac{\partial^2 \ln L(\hat{\boldsymbol{\theta}})}{\partial \hat{\theta}_i \partial \hat{\theta}_j}\right], \tag{13}$$

where $\boldsymbol{\theta}^T = (\alpha, \beta, m)$. If the number of data n is sufficiently large, the covariance matrix $\mathbf{S}(\hat{\boldsymbol{\theta}})$ is equal to the inverse matrix of the Fisher information matrix

$$\mathbf{S}(\hat{\boldsymbol{\theta}}) \equiv \begin{pmatrix} \hat{\sigma}_\alpha^2 & \hat{\sigma}_{\alpha\beta} & \hat{\sigma}_{\alpha m} \\ \hat{\sigma}_{\alpha\beta} & \hat{\sigma}_\beta^2 & \hat{\sigma}_{\beta m} \\ \hat{\sigma}_{\alpha m} & \hat{\sigma}_{\beta m} & \hat{\sigma}_m^2 \end{pmatrix} = \mathbf{H}(\hat{\boldsymbol{\theta}})^{-1}. \tag{14}$$

Using equations (13) and (14), we can estimate variance of the estimated parameters. For α, β,

$$\hat{\sigma}_\beta^2 = \frac{1}{n\hat{m}} \frac{1}{\left\{\frac{E_2}{E_0} - \left(\frac{E_1}{E_0}\right)^2\right\}}, \tag{15}$$

$$\hat{\sigma}_\alpha^2 = \frac{E_0 E_2}{n^2}\hat{\sigma}_\beta^2, \tag{16}$$

$$\hat{\sigma}_{\alpha\beta} = \frac{1}{n^2} \frac{E_1}{\{\frac{E_2}{E_0} - (\frac{E_1}{E_0})^2\}}, \tag{17}$$

$$E_l \equiv \sum_{i=1}^{n} r_i^2 t_i^{k+l} \exp(\hat{\beta} t_i). \tag{18}$$

For m,

$$\hat{\sigma}_m^2 = \frac{1}{n} \frac{1}{\psi'(\hat{m}) - \frac{1}{\hat{m}}}, \tag{19}$$

where $\psi'(\hat{m})$ is the trigamma function defined as

$$\psi'(m) \equiv \frac{d^2 \log \Gamma(m)}{dm^2}. \tag{20}$$

The variance becomes smaller with the number of data n. For the covariance of the parameters, we find

$$\hat{\sigma}_{\alpha m} = \hat{\sigma}_{\beta m} = 0, \tag{21}$$

from which we confirm that α, β are independent of m as we already noted.

Special Probability Plot for Linearizing the Nakagami-m Distribution

It is convenient to make a special probability plot for linearizing the Nakagami-m distribution in order to visually check whether data follow the distribution or not. Here, the method originally proposed by Nakagami (1943) is slightly modified as explained later.

First, we express an amplitude r in a logarithmic scale as

$$z = 10 \log_{10}\left(\frac{r^2}{\Omega}\right). \tag{22}$$

Division by Ω is important as described later. We further transform z to x with care about the sign of z by

$$x \equiv 1 + \frac{z}{10 \log_{10} e} - \exp\left(\frac{z}{10 \log_{10} e}\right) \qquad (z \le 0),$$
$$x \equiv -\left\{1 + \frac{z}{10 \log_{10} e} - \exp\left(\frac{z}{10 \log_{10} e}\right)\right\} \qquad (z \ge 0). \tag{23}$$

Using the transformation and the probability density function in equation (1), we find the following relations:

$$y = mx + c \qquad (x \le 0),$$
$$y = -mx + c \qquad (x \ge 0), \tag{24}$$

where

$$y \equiv \log p(z), \tag{25}$$

$$c \equiv m(\log m - 1) - \log[10\Gamma(m)], \tag{26}$$

and $p(z)$ is the probability density function of the Nakagami-m distribution with respect to z. We can easily see if data

follow the Nakagami-m distribution or not from the linearity on a plot of y against x. From equation (24), we expect a linear relation with a positive slope for $x \leq 0$ and a negative slope for $x \geq 0$. The slope gives the value of m.

For making such a plot from data, we first calculate x_i from an observed amplitude r_i according to equations (22) and (23). We repeat it for all the data, and count the number of data contained in each bin of x. The logarithm of the number is y. We are reminded that the amplitude r is generally time-dependent. But we expect that division by Ω in z tries to remove the time dependence of z. In other words, z is stationarized. Therefore, we do not show explicitly the time dependence of the variables in this subsection and plot all the data in the same plot irrespective of lapse time. We will show an example of the plot in the next section and find that this idea is acceptable.

The transformation of variables was originally proposed by Nakagami (1943). He further devised to fold the data for $x > 0$ upward with respect to $y = y(x = 0)$; in other words, to take the vertical axis in a descending order for $x > 0$, so as to get one straight line on the plot. Though his ingenious method enables us to check the linearity visually and quickly, it seems confusing that the vertical axis changes in the middle of the plot. That is why we modified his method slightly.

Application to Data

The methods described in the Method section are applied to real data. We use three stations at IWTH02, IWTH13, and IWTH17 shown by solid triangles in Figure 3 among the Kik-net, a Japanese nationwide strong-motion network managed by the National Research Institute for Earth Science and Disaster Prevention. At each of the stations, two three-component strong-motion seismometers are installed on the top and the bottom of a borehole with a depth of about 100 m. The seismometers at the bottom at stations IWTH02, IWTH13, IWTH17 are named IWTB02, IWTB13, IWTB17 in this study, respectively. Frequency characteristics of the seismometers are flat in amplitude from direct component to 30 Hz (see the Data and Resources section). Acceleration records are sampled at a rate of 200 Hz. Sixty local events are used in the analysis, whose epicenters are shown by solid stars. The magnitude ranges from 3.3 to 7.1 and epicentral distance is smaller than 200 km.

The three stations are located in Katakami Mountain Range, which is mainly composed of sedimentary and granitic rocks in Paleozoic or Mesozoic time. According to the well-log data, S-wave velocity is higher than 1200 m/s up to a depth of a few meters at IWTH13 and IWTH17, which suggests that the two stations are in good site conditions. However, IWTH02 is in a worse site condition, where a basement with such high S-wave velocity exists deeper at a depth of about 30 m.

First, we integrate original acceleration records into velocity records after baseline correction. Performing band-pass filtering between 1–2, 2–4, 4–8, 8–16, and 16–32 Hz, we calculate amplitude according to equation (2). An example is shown in Figure 2. The envelope is decaying with time with superimposing fast fluctuations.

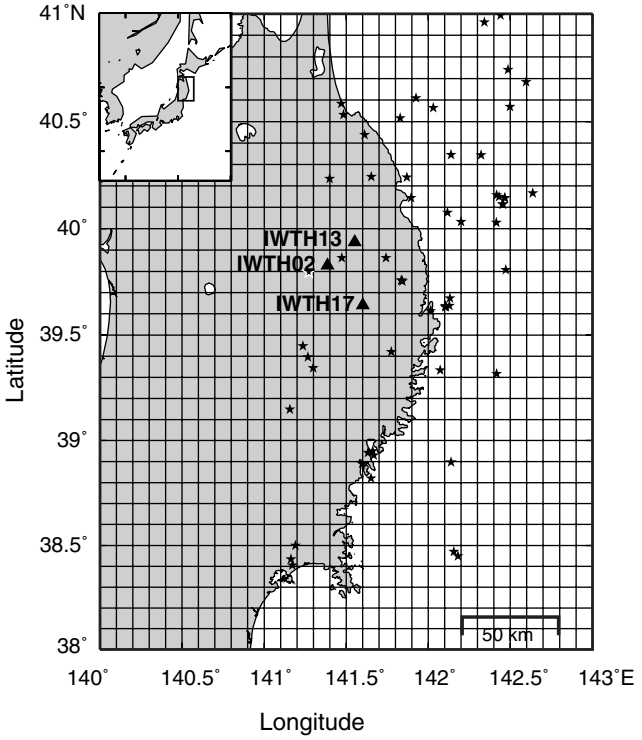

Figure 3. Map of the studied area. Three stations are shown by solid triangles. Epicenters of 60 events used are shown by solid stars. The magnitude ranges from 3.3 to 7.1 and epicentral distance is smaller than 200 km.

In order to visually check if the data shown in Figure 2 obey the Nakagami-m distribution or not, we make a special probability plot in Figure 4 by following the procedures described in the Method section. Two lines with slopes of ± 1 are drawn for reference. The data shown by gray circles linearly increase in negative x, and linearly decrease in positive x, from which we can judge that the data follow the Nakagami-m distribution. And we also know that m is close to 1 from the slope of the data.

For a better quantitative fit, we conduct the maximum-likelihood estimation by assuming a geometrical spreading factor of $k = 2$ for S waves and using a time window from 1.5 times the travel time of direct S wave to a lapse time of 80 s. The 80 s is set such that the time window is longer than 5 s even for the farthest event (the largest direct S-wave travel time is about 50 s). We calculate noise energy for a 2.5 s-long window between 3.5 s before and 1.0 s before the direct P-wave arrival. We also calculate signal energy for a 2.5 s-long time window in lapse times between 77.5 s and 80 s. The data with the signal-to-noise energy ratio smaller than 2 are rejected.

A bisection method (e.g., Press *et al.*, 1992) is adopted to solve equation (9) for β. We assume that β ranges from

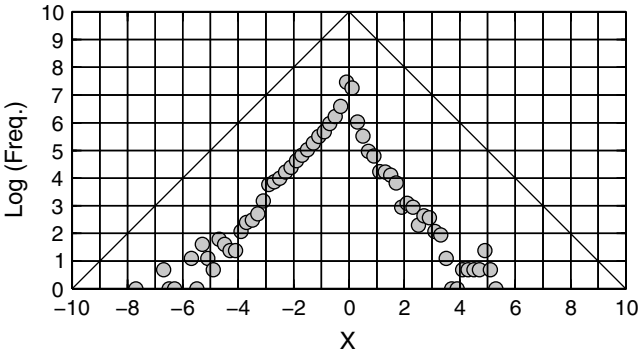

Figure 4. A special probability plot for the Nakagami-m distribution. The horizontal axis is x in equation (23). The vertical axis is the logarithmic frequency of data in each bin of the horizontal axis. Gray circles are data taken from the envelope shown in Figure 2. $x = 0$ is located at the peak of the frequency. Two lines with a slope of ± 1 are drawn for reference.

0 to 1.7. The lower limit is assumed to be 0, because negative coda Q is not physically reasonable. The upper limit of 1.7 is used because the terms in equation (9) will diverge for larger β. We also estimate m by solving equation (11) with the bisection method for a range of m from 0.5 to 5. The lower limit of 0.5 is known theoretically by Nakagami (1960). The upper limit is set because m is smaller than 5 for our observed data. An example of envelope fitting is shown in Figure 5. A thick gray curve is the square root of Ω with $Q_c = 1021.5$, and reproduces a smoothly decaying part of the coda. For the data, m is estimated to be 0.95 ± 0.01.

Such estimations are repeated for all of the events, stations, components, and frequencies of our data set. In Figure 6, inverse values of coda Q (Q_c^{-1}) are plotted. The top three panels show the results on the surface receivers, and the bottom panels show those at the subsurface receivers. Q_c^{-1} changes from about 10^{-2} at 1–2 Hz band to about 5×10^{-4} at 16–32 Hz decreasing with frequency increasing. A slope of Q_c^{-1} versus frequency is about -1. The values are within a range of the compiled values by Carcolé and Sato (2010). And we note that Q_c^{-1} is similar among different components, especially for higher frequencies. We also note

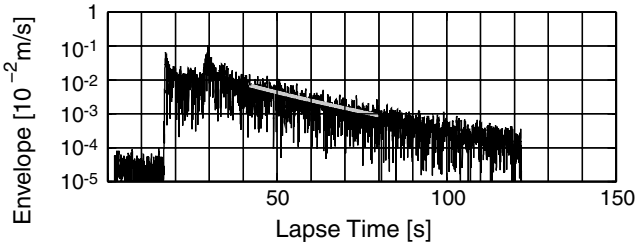

Figure 5. Observed rms envelope is shown by a solid curve for a local earthquake with a magnitude of 5.2 and a hypocentral distance of about 100 km in 8–16 Hz band on the vertical component at IWTH17 station. The synthetic envelope for best α and β according to the ML method is shown by a gray curve, which well reproduces a slowly decaying part of coda.

that Q_c^{-1} is not so different between surface and subsurface receivers.

As an example, variation of m with events is shown in Figure 7. The horizontal axis is an event number assigned according to temporal order of occurrence. We find that variations are large for lower frequencies, and get smaller with increasing frequencies. In Table 1, we list the mean and the one standard deviation of estimated m parameters for all the events. For some events, m is significantly different from 1 as seen in Figure 7. But an average value with respect to the events is generally close to 1 despite large variations.

Discussion

We consider the physical meaning of m. The following relation can be derived for the Nakagami-m distribution (e.g., Nakagami, 1960):

$$m = \frac{\Omega^2}{\sigma_{r^2}^2}. \tag{27}$$

This means that m is inversely proportional to the variance of r^2 denoted as $\sigma_{r^2}^2$, which is an indication of fluctuations in MS envelopes. For larger fluctuations m becomes smaller, and vice versa. In laser propagation, the scintillation index is often used to express the fluctuations in intensity, and the scintillation index is exactly a reciprocal of m. For weak scattering cases, the scintillation index for direct pulsed wave parts can be calculated based on the Rytov approximation (e.g., Andrews and Phillips, 2005). In seismology, Hoshiba (2000) studied the scintillation index by numerical simulations of seismic wave propagation in 3D random velocity structures. He showed how the scintillation index changes with travel distance for different types of the random media. Now that we know a relation between m and the scintillation index, studies on the scintillation index can also be used for the studies on m.

For radio waves, it is pointed out that m is close to 1 for longer travel distances and is greater than 1 for shorter travel distances (e.g., Nakagami, 1943). We look at our data from the same viewpoint. In Figure 8, we show the dependence of m on the direct S-wave travel time T_S, which is roughly proportional to the hypocentral distance. However, a clear tendency is not found on the plot. This might be because the largest travel distance of coda waves is the same for all the events, because we use coda waves up to 80 s in the lapse time for all the events.

In Figures 7 and 8, variations of m are found to become larger for lower frequencies and vice versa. It is important to consider whether the variations are of physical origin or of statistical origin. In this study, we use time windows with the same length for all frequency bands. Therefore, a larger number of waves is contained in the time windows for higher frequencies. Statistical fluctuations (e.g., standard deviations) in the amplitude of incoherent waves are expected to be inversely proportional to a square root of the number

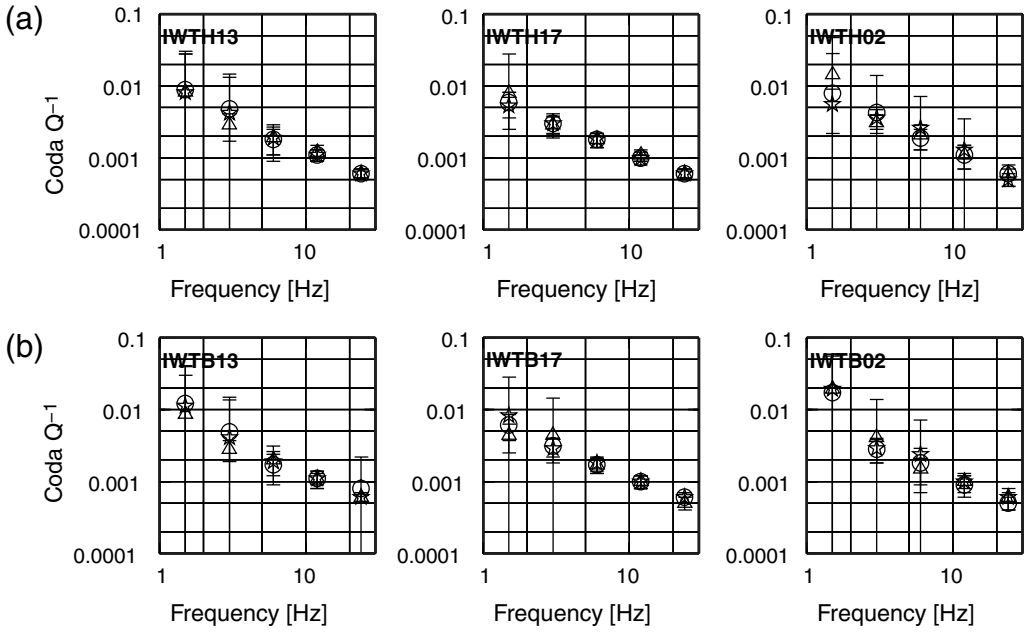

Figure 6. Frequency dependence of estimated coda Q. (a) Three panels are the results at the surface receivers; (b) three panels are those at the subsurface receivers. Circles, triangles, and stars are mean values with respect to the events for vertical, north–south, and east–west components, respectively. Error bars show one standard deviation.

of the waves. Therefore, when the central frequency becomes half, the fluctuations will be larger by a factor of $\sqrt{2}$. If we assume the standard deviation of 0.04 for 16–32 Hz as an example, the square-root dependency estimates the standard deviation of 0.06 for 8–16 Hz, 0.08 for 4–8 Hz, 0.12 for 2–4 Hz, and 0.16 for 1–2 Hz. These values can be compared with the observed standard deviations listed in Table 1. Though the observed deviations might be larger than the expected ones in lower frequencies, especially in 1–2 Hz, both the observations and expectations are comparable for the higher frequencies. Therefore, we think that the variations in m are mainly of statistical origin except in

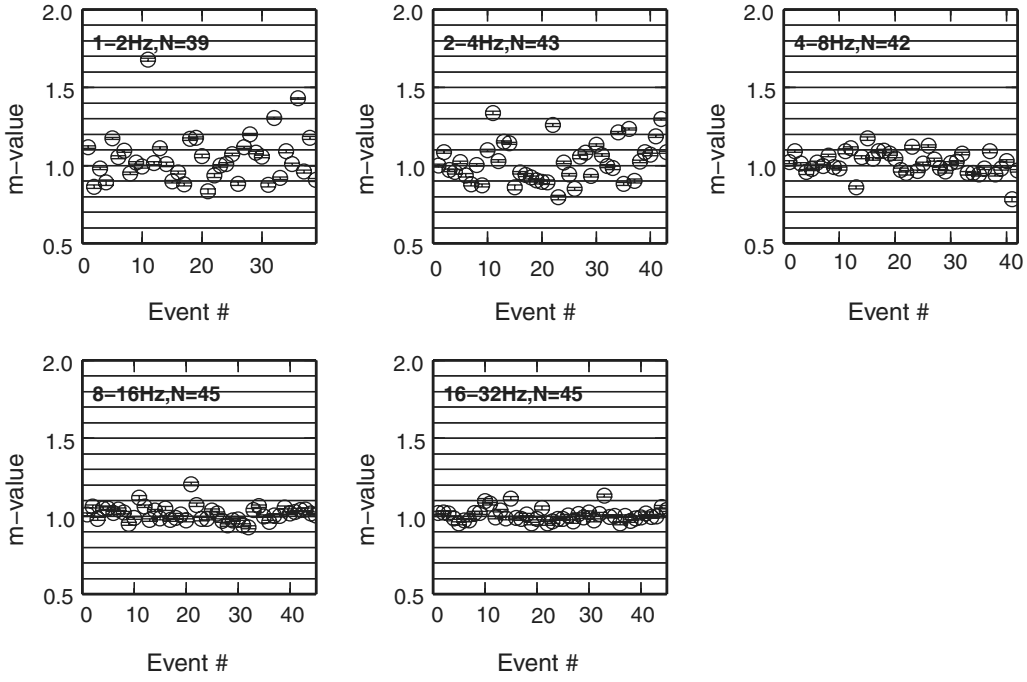

Figure 7. Variations of m with events for vertical components at station IWTH17. The horizontal axis is the event number assigned according to temporal order of occurrence. Open circles are estimated by ML, and error bars show one standard deviation.

Table 1
m-Parameters Estimated

	1–2 Hz	2–4 Hz	4–8 Hz	8–16 Hz	16–32 Hz
(a) IWTH13					
East–west	1.04 ± 0.31	1.04 ± 0.27	1.02 ± 0.07	1.00 ± 0.05	0.99 ± 0.04
North–south	1.12 ± 0.33	1.03 ± 0.10	1.01 ± 0.11	1.01 ± 0.05	1.01 ± 0.06
Vertical	1.09 ± 0.34	1.10 ± 0.39	1.01 ± 0.07	1.01 ± 0.05	1.00 ± 0.04
(b) IWTH17					
East–west	1.05 ± 0.18	1.01 ± 0.08	1.03 ± 0.06	1.01 ± 0.05	0.99 ± 0.05
North–south	1.08 ± 0.31	1.03 ± 0.09	1.01 ± 0.07	1.00 ± 0.05	0.99 ± 0.05
Vertical	1.05 ± 0.16	1.02 ± 0.13	1.01 ± 0.07	1.02 ± 0.05	1.01 ± 0.04
(c) IWTH02					
East–west	1.05 ± 0.16	1.02 ± 0.09	1.08 ± 0.27	1.10 ± 0.27	1.02 ± 0.09
North–south	1.18 ± 0.45	1.04 ± 0.15	1.02 ± 0.11	1.05 ± 0.10	0.99 ± 0.06
Vertical	1.11 ± 0.30	1.06 ± 0.29	1.01 ± 0.08	1.01 ± 0.08	1.01 ± 0.07
(d) IWTB13					
East–west	1.07 ± 0.41	1.05 ± 0.28	1.05 ± 0.09	1.02 ± 0.06	0.99 ± 0.06
North–south	1.12 ± 0.35	1.01 ± 0.10	1.01 ± 0.10	1.01 ± 0.06	1.01 ± 0.06
Vertical	1.13 ± 0.41	1.14 ± 0.41	1.03 ± 0.09	1.01 ± 0.06	1.05 ± 0.30
(e) IWTB17					
East–west	1.09 ± 0.31	1.03 ± 0.11	1.00 ± 0.07	0.99 ± 0.05	1.01 ± 0.04
North–south	1.05 ± 0.17	1.05 ± 0.29	1.02 ± 0.07	0.99 ± 0.06	1.00 ± 0.04
Vertical	1.03 ± 0.14	1.02 ± 0.13	0.99 ± 0.10	0.99 ± 0.06	0.99 ± 0.04
(f) IWTB02					
East–west	1.23 ± 0.54	0.99 ± 0.12	1.04 ± 0.27	1.03 ± 0.07	1.01 ± 0.06
North–south	1.26 ± 0.53	1.06 ± 0.28	1.01 ± 0.11	1.01 ± 0.07	1.02 ± 0.05
Vertical	1.24 ± 0.52	1.02 ± 0.12	1.00 ± 0.09	1.00 ± 0.05	1.00 ± 0.04

frequencies as low as 1–2 Hz, where an assumption of incoherent waves is not always correct and some deterministic regional differences in velocity structures might play a role.

Sometimes seismogram envelopes are not expressed by the simple functional form of equation (3), and anomalous envelopes are identified as ripples (e.g., Kosuga, 1997) or steps and bumps (e.g., Obara, 1997). For such cases, our method may not give correct results because Ω is not explained well by equation (3). Therefore, to get correct values of m, we need to estimate Ω in a different way, for example, by averaging envelopes with a time window sufficiently longer than the fluctuations.

We take an approach to characterize fluctuations in envelopes statistically. On the other hand, there are some studies taking a deterministic approach in terms that each fluctuation in envelopes is projected back to certain spatial regions of strong and weak scattering. For example, Nishigami (1991) developed a method to invert for spatial variations in relative scattering coefficient from the fluctuations in seismogram envelopes. Roughly speaking, the idea is that convex portions of envelopes with respect to a mean envelope correspond to contributions from a stronger scattering area, and concave portions correspond to those from a weaker scattering area. The method has been applied to clarify spatial distribution of scatterers in fault regions (e.g., Nishigami, 2000) and in volcanoes (e.g., Carcolé *et al.*, 2006). To estimate absolute values of scattering coefficients, Asano and Hasegawa (2004) further developed a nonlinear inversion method. We interpret that they used slowly fluctuating parts of envelopes, that is, anomalies in envelopes of Ω, and such parts can be treated deterministically. However, rapidly fluctuating parts of envelopes should be analyzed statistically as shown in this study.

Conclusion

We have proposed a new ML method to simultaneously estimate coda Q and the Nakagami-m parameter from seismogram envelopes. In terms of the estimation of coda Q, we have proved that the previous method of Takahara and Yomogida (1992) proposed for Rayleigh distribution is correct even for the Nakagami-m distribution. In terms of the estimation of the m-parameter, this paper is the first to propose an ML estimation method for seismic waves.

From the data analysis of local earthquakes, we find that coda Q ranges from 100 at 1–2 Hz to 2000 at 16–32 Hz increasing with frequencies increasing. And the values are compatible with previously reported ones. The m-parameter varies with events and is significantly different from 1 for some events. But mean values of m with respect to the events are close to 1 irrespective of components and frequencies. Variations in m are found to be larger for lower frequencies, which is mainly explained by a statistical reason. The m-parameter is exactly equal to a reciprocal of the scintillation index, which quantifies fluctuations in seismogram envelopes. Studies on the m-parameter will help investigate

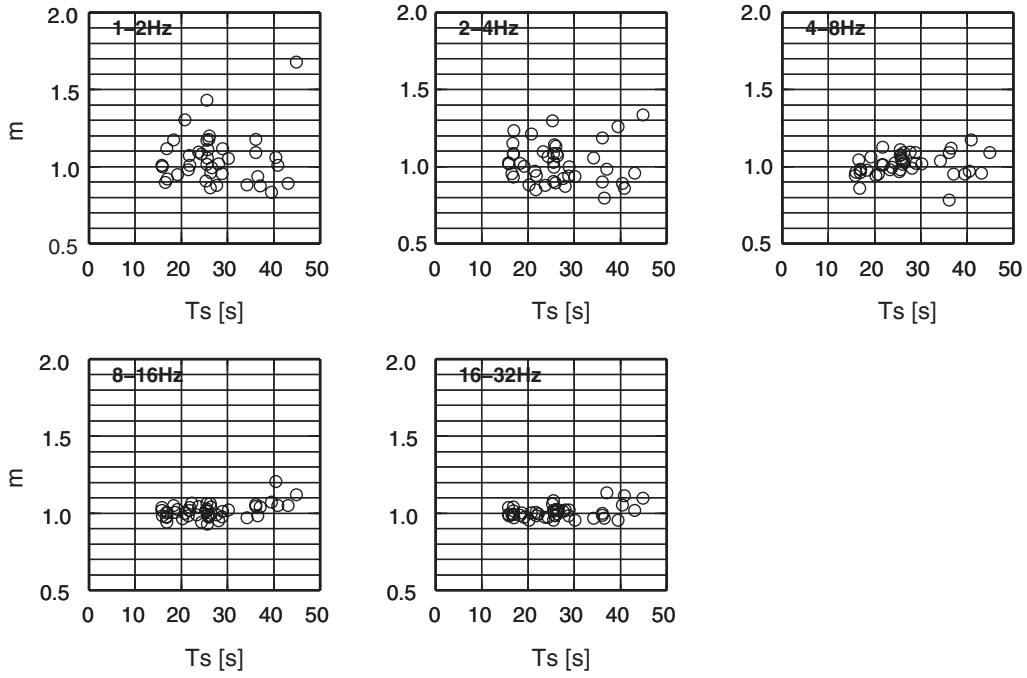

Figure 8. Dependence of m on the direct S-wave travel time V_S for vertical component at station IWTH17. V_S is roughly proportional to the hypocentral distance. Open circles are m estimated by ML.

statistical characteristics of small-scale fluctuations in seismic velocity structure in the Earth.

Data and Resources

Seismograms used in this study can be obtained from the KiK-net, the National Research Institute for Earth Science and Disaster Prevention, Tsukuba, Japan at http://www.kik.bosai.go.jp/kik/index_en.shtml (last accessed May 2010). The frequency characteristics of the KiK-net seismometers can be found at http://www.kik.bosai.go.jp/kik/ftppub/seismo/KiK_characteristics.pdf (last accessed May 2010). An integrated event catalog used in this study was produced by the Japan Meteorological Agency and the Ministry of Education, Culture, Sports, Science and Technology in Japan, and can be downloaded from http://www.hinet.bosai.go.jp/ (last accessed May 2010). Figures were prepared using Generic Mapping Tools (Wessel and Smith, 1998).

Acknowledgments

We are grateful to two anonymous reviewers and associate editor M. Bouchon for helpful comments. This study was partly supported by Grant-in-Aid for Young Scientists (B) (20740248) from the Japan Society for the Promotion of Science. Eduard Carcolé is enjoying a postdoctoral fellowship of the Global COE program for Earth Science in Tohoku University, Sendai, Japan. He also acknowledges the support of the MCYT project CGL2008-00869/BTE.

References

Aki, K., and B. Chouet (1975). Origin of coda waves: Source, attenuation, and scattering effects, *J. Geophys. Res.* 3322–3342.

Andrews, L. C., and R. L. Phillips (2005). *Laser Beam Propagation through Random Media*, Second Ed., SPIE Optical Engineering Press, Bellingham, Washington.

Asano, Y., and A. Hasegawa (2004). Imaging the fault zones of the 2000 Western Tottori earthquake by a new inversion method to estimate three-dimensional distribution of the scattering coefficient, *J. Geophys. Res.* **109,** B06306, doi 10.1029/2003JB002761.

Carcolé, E., and H. Sato (2009). Statistics of the fluctuations of the amplitude of coda waves of local earthquakes, *Abstracts of the Seismological Society of Japan 2009 Fall Meeting*, C31-13, Kyoto, Japan.

Carcolé, E., and H. Sato (2010). Spatial distribution of scattering loss and intrinsic absorption of short-period S waves in the lithosphere of Japan on the basis of the multiple lapse time window analysis of Hi-net data, *Geophys. J. Int.* **180,** 268–290.

Carcolé, E., A. Ugalde, and C. A. Vargas (2006). Three-dimensional spatial distribution of scatterers in Galeras volcano, Columbia, *Geophys. Res. Lett.* **33,** L08307, doi 10.1029/2006GL025751.

Hoshiba, M. (2000). Large fluctuation of wave amplitude produced by small fluctuation of velocity structure, *Phys. Earth Planet. In.* **120,** 201–217.

Karasawa, Y. (2003). *Radiowave Propagation Fundamentals for Digital Mobile Communications*, Corona Publishing Co. Ltd., Tokyo (in Japanese).

Kosuga, M. (1997). Periodic ripple of coda envelope observed in northeastern Japan, *Phys. Earth Planet. In.* **104,** 91–108.

Nakagami, M. (1943). Some statistical characters of short-wave fading, *J. Inst. Elec. Commun. Engrs. Japan*, 145–150 (in Japanese).

Nakagami, M. (1960). The m-distribution, a general formula of intensity distribution of rapid fading, in *Statistical Methods in Radio Wave Propagation*, W. G Hoffman (Editor), Pergamon, Oxford, England.

Nishigami, K. (1991). A new inversion method of coda waveforms to determine spatial distribution of coda scatterers in the crust and upper mantle, *Geophys. Res. Lett.* **18,** 2225–2228.

Nishigami, K. (2000). Deep crustal heterogeneity along and around the San Andreas fault system in central California and its relation to segmentation, *J. Geophys. Res.* **105,** 7983–7998.

Obara, K. (1997). Simulations of anomalous seismogram envelopes at coda portions, *Phys. Earth Planet. In.* **104,** 109–125.

Press, W. H., S. A. Teukolsky, W. T. Vetterling, and B. P. Flannery (1992). *Numerical Recipes in FORTRAN*, Second Ed., Cambridge University Press, New York.

Sato, H., and M. Fehler (1998). *Seismic Wave Propagation and Scattering in the Heterogeneous Earth*, Springer-Verlag, New York.

Takahara, M., and K. Yomogida (1992). Estimation of coda Q using the maximum likelihood method, *PAGEOPH* **139,** 255–268.

Wessel, P., and W. H. F. Smith (1998). New improved version of the Generic Mapping Tools released, *Eos. Trans. AGU* **79,** 579.

Zhang, Q. T. (2002). A note on the estimation of Nakagami-*m* fading parameter, *IEEE Comm. Lett.* **6,** 237–238.

Department of Geophysics
Graduate School of Science
Tohoku University
6-3, Aramaki-Aza-Aoba, Aoba-ku
Sendai 980-8578, Japan
naka@zisin.gp.tohoku.ac.jp

Manuscript received 29 January 2010